

Supporting Information

Mechanism of photocatalytic water splitting with carbon nitrides: Deep mechanistic insights from extensive ab initio calculations for the triazine-water complex

Johannes Ehrmaier,^{1, a)} Mikołaj J. Janicki,^{1, 2} Andrzej L. Sobolewski,³ and Wolfgang Domcke^{1, b)}

¹⁾*Department of Chemistry, Technical University of Munich, D-85748 Garching, Germany*

²⁾*present address: Department of Physical and Quantum Chemistry, Faculty of Chemistry, Wrocław University of Science and Technology, Wybrzeże Wyspiańskiego 27, 50-370, Wrocław, Poland*

³⁾*Institute of Physics, Polish Academy of Sciences, 02-668 Warszawa, Poland*

^{a)}johannes.ehrmaier@tum.de

^{b)}domcke@ch.tum.de

CONTENTS

I. Computational Methods	2
II. Equilibrium Geometry and Vertical Excitation Energies of Triazine	5
III. Vertical Excitation Energies of the Triazine-Water Complex	7
IV. Energy Profiles for H-atom Transfer in the Triazine-Water Complex: Benchmarking the ADC(2) Method	9
V. Vertical Excitation Energies of the Triazinyl Radical	10
VI. PE Functions for H-atom Detachment from the Triazinyl Radical: Benchmarking the ADC(2) Method	11
References	12

I. COMPUTATIONAL METHODS

The ground-state geometry of triazine was optimized using second-order Møller-Plesset perturbation (MP2) theory without symmetry constraints. Singlet and triplet vertical excitation energies of triazine were calculated with the second-order algebraic-diagrammatic-construction method (ADC(2))¹, the second-order approximate coupled-cluster method (CC2)² and the equation-of-motion coupled cluster method with singles and doubles (EOM-CCSD)³ method. In addition, the complete-active-space self-consistent-field (CASSCF)⁴ method with multi-state second-order perturbation theory (multi-state CASPT2) was used.⁵ The active space of the CASSCF calculations for the triazine-H₂O complex consisted of three occupied π orbitals, three occupied n orbitals and three unoccupied π^* orbitals, i.e. 12 electrons in 9 orbitals. This active space involves all π and π^* orbitals of the triazine ring as well as the important n orbitals of the nitrogen atoms. Five states of A' symmetry and six states of A'' symmetry were included in the state averaging with equal weights. For the triplet states, four states of A' and four states of A'' symmetry were included in the state averaging. The standard level-shift of 0.3 au was used in the CASPT2 calculations.

The ground-state geometry of the triazine-water complex was optimized at the MP2 level. The conformer of lowest energy has C_s symmetry, the water molecule being in the molecular plane of triazine. The same methods as for triazine were used for the calculation of the singlet and triplet vertical excitation energies. In this case the active space of the CASSCF calculations comprised four occupied and three virtual π orbitals and three occupied n orbitals, i.e. 14 electrons in ten orbitals. The active space of the triazine molecule has thus been extended by the p_z orbital of water. Five states of A' and six states of A'' symmetry were included in the state averaging in the singlet manifold. For the triplet states, four states of A' and four states of A'' symmetry were included in the state averaging.

To characterize the reaction path for H-atom transfer from water to triazine, a relaxed scan along the OH distance of water which is involved in hydrogen bonding was performed for the $\pi\pi^*$ and $n\pi^*$ states at the ADC(2) level. For fixed OH distance, the energies of the lowest $^1n\pi^*$ and $^1\pi\pi^*$ states were optimized with respect to all other nuclear degrees of freedom. For the lowest $^1n\pi^*$ state, this relaxed scan could also be performed at CASSCF level. For the geometries obtained at the CASSCF level, the energies were calculated at the CASPT2 level. For the CASSCF relaxed scan and the associated CASPT2 calculations, the active space was reduced to ten electrons in ten orbitals to improve the convergence. This active space consists of three π and three π^* orbitals as well as two n and two σ^* orbitals. The CASSCF energy was optimized for the lowest state of A' and A'' symmetry, respectively.

Two-dimensional maps of the lowest $\pi\pi^*/n\pi^*$ singlet and triplet PE surfaces were calculated at the ADC(2) level. For fixed OH and ON distances, the energies of the lowest $^1n\pi^*$ and $^1\pi\pi^*$ states were optimized with respect to the remaining nuclear degrees of freedom. In these calculations the three CH bond lengths had to be kept fixed to suppress undesired side reactions (such as H-atom abstraction by OH radicals).

Linearly interpolated reaction paths (LIRPs) between the ground-state equilibrium geometry and the geometry optimized for the $\pi\pi^*$ and $n\pi^*$ states at $R_{\text{OH}} = 1.2 \text{ \AA}$ were constructed by linear interpolation in Cartesian coordinates. At the interpolated geometries single-point ADC(2) calculations are performed.

The ground-state geometry of the triazinyl radical was optimized at the unrestricted MP2 (UMP2) level without symmetry constraints. The vertical excitation energies of the triazinyl radical were calculated using the ADC(2), CC2, EOM-CCSD, CASSCF and CASPT2 methods. The ADC(2), CC2 and EOM-CCSD calculations were based on unrestricted Hartree-Fock (UHF) calculations. The active space for the CASSCF calculations of the vertical excitation energies consisted of three doubly occupied π orbitals, the singly occupied π orbital and two unoccupied π^* orbitals. In addition, one occupied n orbital and seven σ^* orbitals were included, in total 9 electrons in 14 orbitals. It was shown earlier for the pyridinyl radical that an active space with many virtual σ^* orbitals is necessary to describe the dense set of electronic excitations appropriately, since in most low-lying excitations the electron of the singly occupied π orbital is promoted to a σ^* orbital.⁶ Three states of A'' and eight states of A' symmetry were included in the state averaging. Due to convergence difficulties, only CASPT2 (rather than multi-state CASPT2) calculations could be performed.

To characterize the photoinduced detachment of the H-atom from the triazinyl radical, a rigid scan along the NH distance was calculated. The scan was performed at the ADC(2) and CASSCF/CASPT2 levels. For the CASSCF/CASPT2 calculations, the active space consisted of three occupied n and three unoccupied σ^* orbitals as well as three doubly occupied π , the singly occupied π and two virtual π^* orbitals.

All calculations, except the multi-state CASPT2 calculations for triazine and triazine-H₂O, were performed with the augmented correlation-consistent double- ζ basis set (aug-cc-pVDZ).⁷ Due to convergence problems, the basis set for the multi-state CASPT2 calculations had to be reduced to the correlation-consistent double ζ basis set without augmentation (cc-pVDZ). Moreover, all calculations were performed under C_s symmetry constraint, except optimizations of the equilibrium geometries of triazine, triazine-water and triazinyl. The MP2 and ADC(2) calculations were performed with the Turbomole program package (V6.3.1).⁸ The resolution-of-identity (RI) approximation⁹ was used for the evaluation of two-electron integrals. Gaussian¹⁰ was used for the EOM-CCSD calculations. The CASSCF and CASPT2 calculations were performed with Molpro¹¹.

II. EQUILIBRIUM GEOMETRY AND VERTICAL EXCITATION ENERGIES OF TRIAZINE

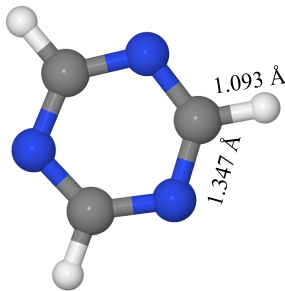


FIG. S1: Geometry of the pure triazine molecule optimized at the MP2 level.

Fig. S1 shows the optimized geometry of the triazine molecule. The molecule is planar with CN distances of 1.347 Å and CH bond lengths of 1.093 Å. The geometry is in good agreement with the geometry reported by Pyckhout et al. with CN distances of 1.338 Å and CH distances of 1.106 Å, measured via electron diffraction.¹⁴

Tab. SI summarizes the seven lowest singlet vertical excitation energies of triazine obtained at different levels of theory. The ordering of the states is the same as in the benchmark study of Ref. 12. The lowest three singlet states ($1^1A_1'$, $1^1A_2'$ and $1^1E''$) correspond to transitions of an electron from an e' orbital ($17a'/18a'$) to an e'' orbital ($4a''/5a''$) orbital ($n\pi^*$ excitations). The states $1^1A_2'$, $2^1A_2'$ and $1^1E'$ correspond to $e'' \rightarrow e''$ ($2a''/3a'' \rightarrow 4a''/5a''$) $\pi\pi^*$ excitations. Both sets consist of E , A_1 and an A_2 excited states. The $2^1E''$ state, which does not belong to either of these sets, is, according to the ADC(2) calculations, energetically below the $1^1E'$ state.

The energies calculated with the different methods agree reasonably well. The largest differences occur for the energy of the $2^1A_1'$ state. The CASPT2 energy of this state is about 0.2 - 0.4 eV lower than the energy predicted by the other methods. The benchmark calculations of Schreiber et al. and the present CASPT2 results predict the $1^1A_2'$ state energetically

TABLE SI: Vertical excitation energies of singlet states of triazine (in eV) with oscillator strengths f (multiplied by 10). The table also contains the character and the dominant orbital transitions of each state.

state	$1^1A_1''$	$1^1A_2''$	$1^1E''$	$1^1A_2'$	$2^1A_1'$	$1^1E'$	$2^1E''$
character	$n\pi^*$	$n\pi^*$	$n\pi^*$	$\pi\pi^*$	$\pi\pi^*$	$\pi\pi^*$	$n\pi^*$
orbital transitions	$18a' \rightarrow 4a''$ $17a' \rightarrow 5a''$	$18a' \rightarrow 5a''$ $17a' \rightarrow 4a''$	$17a' \rightarrow 5a''$ $18a' \rightarrow 4a''$ $17a' \rightarrow 4a''$ $18a' \rightarrow 5a''$	$3a'' \rightarrow 4a''$ $2a'' \rightarrow 5a''$	$2a'' \rightarrow 4a''$ $3a'' \rightarrow 5a''$	$2'' \rightarrow 5a''$ $3a'' \rightarrow 4a''$ $3a'' \rightarrow 5a''$ $2a'' \rightarrow 4a''$	$18a' \rightarrow 6a''$ $17a' \rightarrow 6a''$
ADC(2)	4.51 (0.00)	4.65 (0.14)	4.61 (0.00)	5.70 (0.00)	7.08 (0.00)	7.72 (4.55)	7.66 (0.00)
CC2	4.59 (0.00)	4.72 (0.15)	4.68 (0.00)	5.77 (0.00)	7.23 (0.00)	7.85 (4.34)	7.68 (0.00)
EOM-CCSD	4.84 (0.00)	4.92 (0.16)	4.92 (0.00)	5.76 (0.00)	7.26 (0.00)	8.01 (4.88)	8.08 (0.00)
CASPT2	4.36	4.57	4.58	5.64	6.87	-	-
CASPT2 ¹²	4.60	4.66 (0.21)	4.71	5.79	7.25 (0.09)	7.49 (6.80)	7.72
Exp. ¹³	-	4.59 (0.13)	3.97	5.70	6.86	7.76 (7.3)	6.15

below the $1^1E''$ state,¹² whereas ADC(2) and CC2 put the $1^1A_2''$ state above the $1^1E''$ state, which seems to be in agreement with experiment. The energetic ordering of the $1^1E'$ and $2^1E''$ states also is not consistent among the computational methods.

Tab. SII gives the lowest six triplet excitation energies of triazine. The energies calculated with the different methods agree reasonably well. The energies predicted by CASPT2 are systematically lower by 0.1 - 0.2 eV than the predictions of the other methods. Comparing triplet energies with singlet energies, the A_2'' and E'' triplet energies are red shifted, whereas the triplet A_1'' energy is blue shifted. In the $\pi\pi^*$ set, the triplet A_1' and E' energies are red shifted, whereas the A_2' energy is blue shifted. Due to these shifts, the ordering of the energies within the two sets of states, ($1^3A_2''$, $1^3E''$ and $1^3A_1''$) and ($1^3A_1'$, $1^3E'$ and $1^3A_2'$), is different from the singlet case.

TABLE III: Vertical excitation energies of triplet states of triazine (in eV). The table also contains the character and the dominant orbital transitions of each state.

state	$1^3A_2''$	$1^3E''$	$1^3A_1''$	$1^3A_1'$	$1^3E'$	$1^3A_2'$
character	$n\pi^*$	$n\pi^*$	$n\pi^*$	$\pi\pi^*$	$\pi\pi^*$	$\pi\pi^*$
orbital transition	$18a' \rightarrow 5a''$ $17a' \rightarrow 4a''$	$17a' \rightarrow 4a''$ $18a' \rightarrow 5a''$ $18a' \rightarrow 4a''$ $17a' \rightarrow 5a''$	$17a' \rightarrow 5a''$ $18a' \rightarrow 4a''$	$2a'' \rightarrow 4a''$ $3a'' \rightarrow 5a''$	$3a'' \rightarrow 5a''$ $2a'' \rightarrow 4a''$ $3a'' \rightarrow 4a''$ $2a'' \rightarrow 5a''$	$2a'' \rightarrow 5a''$ $3a'' \rightarrow 4a''$
ADC(2)	4.23	4.35	4.52	4.95	5.70	6.54
CC2	4.27	4.41	4.59	4.97	5.76	6.68
EOM-CCSD	4.43	4.59	4.83	4.59	5.57	6.52
CASPT2	4.05	4.18	4.36	4.82	5.52	-

III. VERTICAL EXCITATION ENERGIES OF THE TRIAZINE-WATER COMPLEX

The ten lowest vertical excitation energies (excluding Rydberg states) of the triazine-water complex are shown in Tab. SIII. The singlet states are ordered according to the energies calculated with ADC(2). While water itself does not exhibit excited electronic states below 7.20 eV,¹⁵ the complexation of triazine with a water molecule reduces the symmetry and shifts the excited states of triazine. We first focus on the ADC(2) results. Later, we compare them with the results of the other electronic-structure methods. The four lowest singlet excited states are of $n\pi^*$ character. S_3 and S_4 correspond to the degenerate $1^1E''$ state of triazine. Complexation with water lifts the degeneracy of the $1^1E''$ state by 0.03 eV. S_7/S_8 and S_9/S_{10} also correspond to degenerate states of triazine. Their degeneracies are lifted by 0.01 eV and 0.14 eV, respectively, in the triazine-water complex. According to ADC(2), S_7 and S_8 are lower in energy than S_9 and S_{10} , that is, the ordering of these states is interchanged by the complexation with water (blue shift of $n\pi^*$ states). The lowest water-to-triazine charge-transfer (CT) state is at 7.84 eV and corresponds to the transfer

TABLE III: Vertical singlet excitation energies of singlet states (in eV) of the triazine-water complex with oscillator strengths f (multiplied by 10). The character and the dominant orbital transitions of each state and assignment to the states to the corresponding states of triazine are indicated.

state	S_1	S_2	S_3	S_4	S_5	S_6	S_7	S_8	S_9	S_{10}
symmetry	A''	A''	A''	A''	A'	A'	A'	A'	A''	A''
character	$n\pi^*$	$n\pi^*$	$n\pi^*$	$n\pi^*$	$\pi\pi^*$	$\pi\pi^*$	$\pi\pi^*$	$\pi\pi^*$	$n\pi^*$	$n\pi^*$
corr. state in triazine	$1^1A_1'$	$1^1A_2'$	$1^1E''$	$1^1E''$	$1^1A_2'$	$2^1A_1'$	$1^1E'$	$1^1E'$	$2^1E''$	$2^1E''$
orbital transitions	$22a' \rightarrow 5a''$	$22a' \rightarrow 6a''$	$21a' \rightarrow 5a''$	$21a' \rightarrow 6a''$	$4a'' \rightarrow 5a''$ $3a'' \rightarrow 6a''$	$3a'' \rightarrow 5a''$ $4a'' \rightarrow 6a''$	$4a'' \rightarrow 5a''$ $3a'' \rightarrow 6a''$	$3a'' \rightarrow 5a''$ $4a'' \rightarrow 6a''$	$22a' \rightarrow 7a''$	$21a' \rightarrow 7a''$
ADC(2)	4.48 (0.00)	4.60 (0.05)	4.73 (0.05)	4.77 (0.03)	5.70 (0.00)	7.08 (0.02)	7.65 (3.32)	7.66 (3.60)	7.73 (0.00)	7.87 (0.00)
CC2	4.56 (0.00)	4.68 (0.05)	4.81 (0.05)	4.84 (0.03)	5.77 (0.00)	7.24 (0.03)	7.79 (3.14)	7.85 (2.43)	7.77 (0.00)	7.91 (0.00)
EOM-CCSD	4.80 (0.00)	4.91 (0.07)	5.04 (0.06)	5.09 (0.02)	5.77 (0.00)	7.26 (0.00)	8.02 (4.71)	8.03 (5.64)	8.42 (0.00)	8.54 (0.00)
CASPT2	4.94	4.97	5.00	5.06	5.66	6.95	-	-	8.13	8.16

of an electron from the p_z orbital of water ($2a''$) to the $6a''$ orbital located on the triazine ring.

Comparing the different methods, the CC2 and ADC(2) methods give essentially identical results. For the lower states ($S_1 - S_6$), the differences between the EOM-CCSD, ADC(2) and CC2 methods are smaller than 0.32 eV. For the higher states ($S_7 - S_{10}$), the energetical ordering of the states given by the ADC(2) and EOM-CCSD methods is the same, albeit energy differences up to 0.69 eV exist. The CASPT2 energies are in very good agreement with the EOM-CCSD results for the lowest five states. CASPT2 seems to underestimate the energy of the S_6 ($\pi\pi^*$) state. The CASPT2 energies for S_9 and S_{10} are in between the ADC(2) and EOM-CCSD energies. S_7 and S_8 are not reasonably described by the CASPT2 method with the chosen active space.

Tab. SIV shows the vertical excitation energies of the triplet states of the triazine water-complex. For the $n\pi^*$ excited states the energetic shift relative to the singlet states is < 0.4 eV (at the ADC(2) level), while it is approximately 2.0 eV for the $\pi\pi^*$ states. Comparing the different methods, the location of the lowest $^3A'$ state is not the same. ADC(2), CC2 and CASPT2 locate it at the fifth position in energy, whereas EOM-CCSD predicts the lowest $^3A'$ state as the third triplet excitation.

Oliva et al.¹⁶ investigated the absorption spectrum of triazine in liquid water. They ob-

TABLE SIV: Vertical triplet excitation energies of triplet states (in eV) of the triazine-water complex. The character and the dominant orbital transitions of each state and assignment to the states to the corresponding states of triazine are indicated.

state	T_1	T_2	T_3	T_4	T_5	T_6	T_7	T_8
symmetry	A''	A''	A''	A''	A'	A'	A'	A'
character	$n\pi^*$	$n\pi^*$	$n\pi^*$	$n\pi^*$	$\pi\pi^*$	$\pi\pi^*$	$\pi\pi^*$	$\pi\pi^*$
corr. state in triazine	$1^3A'_2$	$1^3E''$	$1^3E''$	$1^3A'_1$	$1^3A'_1$	$1^3E'$	$1^3E'$	$1^3A'_2$
orbital transitions	$22a' \rightarrow 6a''$	$22a' \rightarrow 5a''$	$21a' \rightarrow 5a''$	$21a' \rightarrow 6a''$	$3a'' \rightarrow 5a''$ $4a'' \rightarrow 6a''$	$3a'' \rightarrow 5a''$ $4a'' \rightarrow 6a''$	$4a'' \rightarrow 5a''$ $3a'' \rightarrow 6a''$	$3a'' \rightarrow 6a''$ $4a'' \rightarrow 5a''$
ADC(2)	4.24	4.35	4.46	4.62	4.97	5.70	5.71	6.53
CC2	4.29	4.41	4.52	4.70	4.99	5.76	5.78	6.68
EOM-CCSD	4.46	4.60	4.71	4.92	4.61	5.58	5.60	6.53
CASPT2	4.10	4.21	4.29	4.44	4.85	5.53	5.55	-

served two peaks of similar intensity, one at 4.8 eV and one at 6.0 eV. The first peak can be assigned to the S_2 , S_3 and S_4 states. In isolated triazine, the dipole excitation to the $1^1E''$ state is symmetry forbidden, but complexation with water reduces the symmetry and photoexcitation to the $1^1E''$ state may become weakly allowed. The second peak can probably be assigned to S_5 . The water environment may lead to a blue shift of $n\pi^*$ excitations and the oscillator strength can be enhanced.

IV. ENERGY PROFILES FOR H-ATOM TRANSFER IN THE TRIAZINE-WATER COMPLEX: BENCHMARKING THE ADC(2) METHOD

Fig. S2 shows the energy profiles of singlet states for the relaxed scan for H-atom transfer from water to triazine. The energies of Fig. S2(a) were computed at the CASSCF level, those of Fig. S2(b) at the CASPT2 level. To the left of the dashed vertical line, the geometry has been optimized in the electronic ground state, while the right of the dashed vertical line the geometry has been optimized for the lowest $^1p_{x,y}\pi^*$ CT state (both at the CASSCF level). At the CASSCF level, the intersection of the energy of the $^1p_{x,y}\pi^*$ (CT)

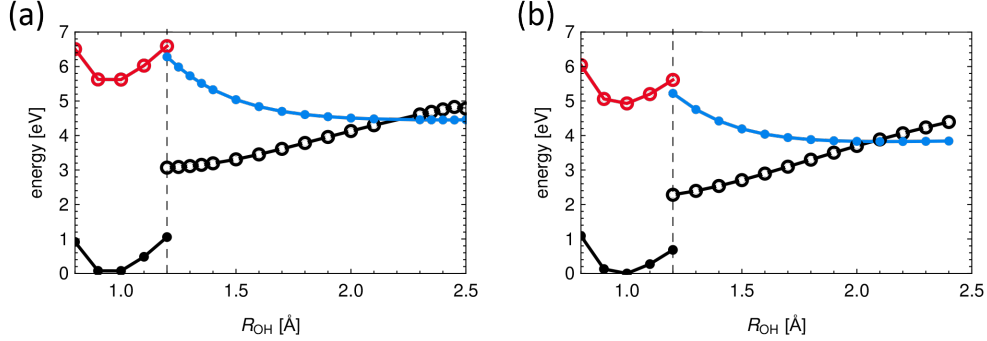


FIG. S2: (a) Relaxed scan for the H-atom transfer from water to triazine at CASSCF level in the triazine-water complex. The S_0 state is shown in black, the ${}^1n\pi^*$ (LE) state in red, the ${}^1p_{x,y}\pi^*$ CT state in blue. Full circles represent energies where the geometry has been optimized in this state. Open circles indicate energies of electronic states that have been optimized in a different electronic state. The dashed vertical line separates the two regions, where the geometry has been optimized in the electronic ground-state (left) and the lowest ${}^1p_{x,y}\pi^*$ CT state (right). (b) Relaxed scan for the H-atom transfer from water to triazine at CASPT2 level.

state with the energy of the S_0 state is at $R_{OH} = 2.2 \text{ \AA}$. The energy minimum of the ${}^1p_{x,y}\pi^*$ (CT) state is at 4.5 eV. Inclusion of dynamical electron correlation via CASPT2 leads to a red shift of the excitation energies and a shift of the ${}^1p_{x,y}\pi^*$ (CT) - S_0 intersection towards smaller OH distances, $R_{OH} = 2.06 \text{ \AA}$. The energy minimum of the ${}^1p_{x,y}\pi^*$ (CT) state is at 3.9 eV. At the ADC(2) level (Fig. 3 in the article), the CI is located at an OH distance of 1.76 \AA and the asymptotic limit is about 1 eV lower than the CASPT2 result. Although the ADC(2) method is not quantitatively accurate for large OH distances, where the electronic ground state is of biradical character, ADC(2) seems acceptable for qualitative studies of the H-atom transfer dynamics.

V. VERTICAL EXCITATION ENERGIES OF THE TRIAZINYL RADICAL

Tab. SV gives the vertical excitation energies of the lowest ten electronic states of the triazinyl radical calculated at different levels of theory. The energies of the ADC(2), CC2 and EOM-CCSD methods differ by less than 0.2 eV. While the CASPT2 energies agree very well with the results of the single-reference methods for $D_2 - D_7$, the CASPT2 energy of D_1 is about 0.4 eV lower than the energy obtained with the EOM-CCSD method. Due

TABLE SV: Vertical excitation energies (in eV) of the triazinyl radical with oscillator strength f (multiplied by 10).

name	D_1	D_2	D_3	D_4	D_5	D_6	D_7	D_8	D_9	D_{10}
symmetry	A''	A'	A'	A'	A''	A'	A'	A'	A'	A'
character	$\pi\pi^*$	$\pi\sigma^*$	$\pi\sigma^*$	$\pi\sigma^*$	$\pi\pi^*$	$\pi\sigma^*$	$\pi\sigma^*$	$\pi\sigma^*$	$n\pi^*$	$\pi\sigma^*$
ADC(2)	1.81 (0.03)	2.85 (0.00)	3.90 (0.00)	3.92 (0.00)	4.19 (0.06)	4.41 (0.02)	4.53 (0.09)	4.67 (0.00)	4.82 (0.00)	5.09 (0.00)
CC2	1.64 (0.03)	2.74 (0.00)	3.80 (0.00)	3.81 (0.00)	4.07 (0.07)	4.41 (0.05)	4.47 (0.05)	4.57 (0.00)	4.67 (0.00)	4.97 (0.00)
EOM-CCSD	1.71 (0.04)	2.92 (0.00)	3.99 (0.00)	4.02 (0.00)	4.20 (0.08)	4.60 (0.00)	4.65 (0.10)	4.66 (0.00)	4.73 (0.00)	5.09 (0.02)
CASPT2	1.34	2.78	3.93	3.94	4.05	4.59	4.64	-	-	-

to limitations of the active space, CASPT2 energies are only listed up to D_7 . States with significant oscillator strength are found at higher energies, e.g. at 5.75 eV with $f = 0.03$ at the ADC(2) level.

VI. PE FUNCTIONS FOR H-ATOM DETACHMENT FROM THE TRIAZINYL RADICAL: BENCHMARKING THE ADC(2) METHOD

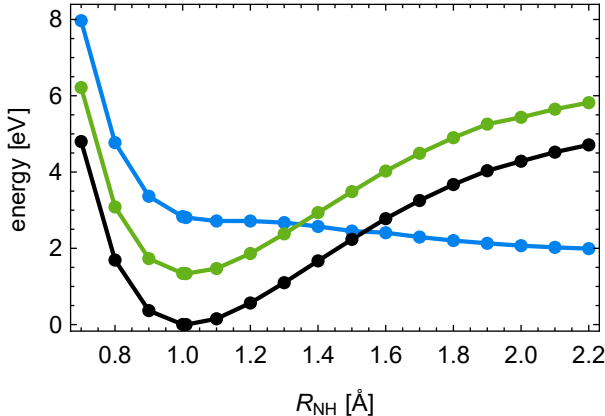


FIG. S3: Rigid scan along the NH distance calculated with the CASSCF method to characterize the H-atom detachment from the triazinyl radical. Black: ground-state, green: ${}^2\pi\pi^*$ state, blue: ${}^2\pi\sigma^*$ state

Fig. S3 shows the CASSCF energies of triazinyl along the H-atom detachment coordinate (rigid scan) for the ground state (black), the ${}^2\pi\sigma^*$ state (blue) and the lowest ${}^2\pi\pi^*$ state (green). The ${}^2\pi\sigma^*$ state is dissociative with respect to the NH stretching coordinate. Its energy curve crosses the energy curve of the lowest ${}^2A''$ $\pi\pi^*$ state at $R_{\text{NH}} = 1.11 \text{ \AA}$ and the ground-state energy curve at $R_{\text{NH}} = 1.49 \text{ \AA}$. The dissociation energy of the ${}^2\pi\sigma^*$ state is

estimated as 1.3 eV at the CASSCF level. Fig. 8(b) of the main paper shows the same PE curves at the CASPT2 level. The A'' states (green) are red-shifted by the inclusion of dynamical electronic correlation energy. The crossing of the energy curves of the lowest ${}^2\pi\pi^*$ state and the reactive ${}^2\pi\sigma^*$ state is at $R_{\text{NH}} = 1.35 \text{ \AA}$. The location of the crossing of the energy profiles of the ${}^2\pi\sigma^*$ state and the D_0 state is less affected by dynamical electron correlation. The low barrier of the CASSCF energy profile of the ${}^2\pi\sigma^*$ state is removed when dynamical electron correlation is included. The dissociation energy of the triazinyl radical is estimated as 2.0 eV at the CASPT2 level, which is 0.7 eV higher than the CASSCF result. For $R_{\text{NH}} = 4.0$, i.e. for separated triazine and H-atom, the lowest vertical excitation energy is 4.39 eV at CASPT2 level, which is in excellent agreement with the excitation energy calculated at CASPT2 level at the equilibrium geometry of isolated triazine. Therefore the CASPT2 PE profile of the ${}^2\pi\sigma^*$ state seems to be accurate.

REFERENCES

- ¹J. Schirmer, *Phys. Rev. A*, 1982, **26**, 2395–2416.
- ²O. Christiansen, H. Koch, and P. Jørgensen, *Chem. Phys. Lett.*, 1995, **243**, 409–418.
- ³H. Koch and P. Jo, *J. Chem. Phys.*, 1990, **93**, 3333–3344.
- ⁴R. Shepard, *Adv. Chem. Phys.*, 1987, **69**, 63–200.
- ⁵B. O. Roos and K. Andersson, *Chem. Phys. Lett.*, 1995, **245**, 215–223.
- ⁶J. Ehrmaier, D. Picconi, T. N. Karsili, and W. Domcke, *J. Chem. Phys.*, 2017, **146**, 124304.
- ⁷T. H. Dunning, *J. Chem. Phys.*, 1989, **90**, 1007.
- ⁸TURBOMOLE V6.3.1 2011, a development of University of Karlsruhe and Forschungszentrum Karlsruhe GmbH, 1989-2007, TURBOMOLE GmbH, since 2007; available from <http://www.turbomole.com>.
- ⁹C. Hättig and F. Weigend, *J. Chem. Phys.*, 2000, **113**, 5154.
- ¹⁰M. J. Frisch, G. W. Trucks, H. B. Schlegel, et al., Gaussian09 Revision E.01.
- ¹¹H.-J. Werner, P. J. Knowles, G. Knizia, F. R. Manby, M. Schütz, et al., Molpro, version 2012.1, a package of ab initio programs, 2012.
- ¹²M. Schreiber, M. R. Silva-Junior, S. P. A. Sauer, and W. Thiel, *J. Chem. Phys.*, 2008,

128, 134110.

¹³A. Bolovinos, P. Tsekeris, J. Philis, E. Pantos, and G. Andritsopoulos, *J. Mol. Spectrosc.*, 1984, **103**, 240–256.

¹⁴W. Pyckhout, I. Callaerts, C. Van Alsenoy, H. Geise, A. Almenningen, and R. Seip, *J. Mol. Struct.*, 1986, **147**, 321–329.

¹⁵N. W. Winter, W. A. Goddard III, and F. W. Bobrowicz, *J. Chem. Phys.*, 1975, **62**, 4325.

¹⁶J. M. Oliva, M. Azenha, H. D. Burrows, R. Coimbra, J. S. Seixas de Melo, L. Canle, M. I. Fernández, J. A. Santaballa, L. Serrano-Andrés, et al., *ChemPhysChem*, 2005, **6**, 306–314.